



ACCOUNTING FOR MOLECULAR ABSORPTION WITHIN THE SPECTRAL RANGE OF THE CERES WINDOW CHANNEL

DAVID P. KRATZ^{†‡} and FRED G. ROSE[§]

[†] Atmospheric Sciences Division, NASA Langley Research Center, Hampton, VA 23681-0001, U.S.A. and

[§] Analytical Services and Materials, Inc., Hampton, VA 23666, U.S.A.

(Received 25 August 1997)

Abstract—Infrared active molecular species residing within the atmosphere cause the emerging thermal infrared spectrum of the Earth to be characterized by both line and continuum absorption (emission). Accounting for the molecular absorption within the atmosphere is critical for the proper interpretation of the satellite measured radiances. Thus, correlated *k*-distribution procedures have been created to account for the molecular line absorption located within the spectral range of the Clouds and the Earth's Radiant Energy System (CERES) infrared window channel (8–12 μm). The derivation of the correlated *k*-distributions is based upon an exponential sum fitting of transmissions (ESFT) procedure that has been applied to monochromatic calculations at predetermined reference pressure and temperature conditions. In addition, an empirically derived, yet highly accurate parameterization of the CKD-2.1 code has been developed to calculate the atmospheric absorption attributed to the water vapor continuum located within the spectral range of the CERES infrared window channel. The multiplication transmissivity approximation has been employed to account for the overlap of the spectral features of different molecular species. The accuracy of the radiative transfer procedures incorporating the correlated *k*-distribution routines and the parameterized CKD-2.1 continuum routines has been established through comparisons with the reference monochromatic procedures. The correlated *k*-distribution yields an upwelling top of atmosphere (TOA) flux for the midlatitude summer (MLS) atmosphere that is within 0.1% of the monochromatic procedures for the CERES window channel. Neglecting the contributions from all the molecular species in the correlated *k*-distribution except H₂O and O₃ yields an upwelling TOA flux for the MLS atmosphere with a 1.5% overestimation. Under circumstances where rapid processing is extremely critical, an error of this magnitude may be deemed acceptable. Neglecting the contributions from all of the molecular species yields an upwelling TOA flux for the MLS atmosphere with a 17.7% overestimation. An error of this magnitude is certainly not acceptable but does emphasize the need to account for the molecular absorption within the spectral range of the CERES window channel instrument. Published by Elsevier Science Ltd.

1. INTRODUCTION

Establishing the radiative effect of molecular absorption (emission) in the atmosphere is essential to the proper interpretation of satellite measured radiances. Since the spectral characteristics of molecular absorption can be highly dependent upon wavenumber, and since satellite instruments produce prodigious amounts of data, an initiative has been undertaken to construct economical parameterizations that will account for the molecular absorption located in the spectral ranges of several satellite radiometers. Because of its efficiency and accuracy in calculating the molecular absorption for nonhomogeneous paths, the correlated *k*-distribution procedure has proven to be an effective parameterization.^{1,2} A further advantage of the correlated *k*-distribution procedure is its ability to be directly incorporated into radiative transfer routines that consider multiple scattering, as well as absorption, by clouds and aerosol particles.

[‡] To whom all correspondence should be addressed.

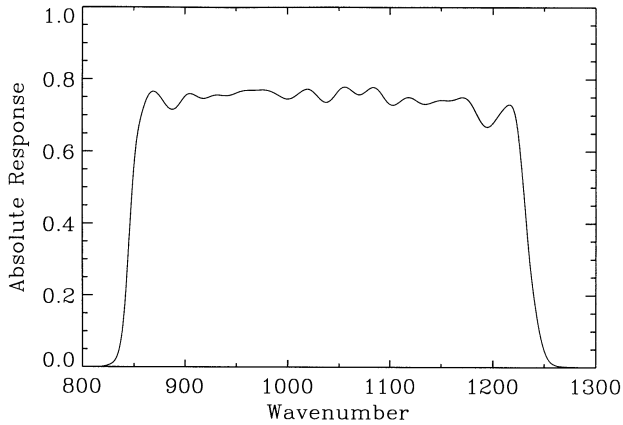


Fig. 1. The spectral response function for the CERES window channel adapted from Lee et al.³ Wavenumber is given in units of cm^{-1} .

The present study focuses upon the production of correlated k -distribution routines created to represent the molecular absorption located within the spectral range from 835 to 1250 cm^{-1} (8–12 μm), an interval which corresponds to the Clouds and the Earth's Radiant Energy System (CERES) window channel (see Fig. 1 adapted from Ref. 3). The CERES endeavor is a critical part of NASA's earth observing system (EOS), with the top of the atmosphere (TOA) radiances measured by the CERES window channel being vital to the retrieval of the surface radiation budget.⁴ CERES window channel measurements also provide a measure of the trace gas radiative forcing under clear sky conditions. Recent anthropogenic activities have led to substantial increases in several trace gas abundances, such as: CO_2 , N_2O , CH_4 , and the CFC's, emphasizing the need to understand the radiative forcing of these trace gases. Additional information gathered by the CERES instrument is crucial for advancing our understanding of cloud-radiation interactions, specifically the impact of cloud feedbacks upon the radiation balance of the earth. Furthermore, CERES data are extremely important for detecting, monitoring, and understanding the processes responsible for the variability of the climate on both regional and global scales. The correlated k -distribution routines reported here will facilitate the understanding of the processes affecting the TOA radiances measured by the CERES window channel instrument.

The derivation of the correlated k -distribution routines for the CERES window channel is based upon well-established line-by-line and narrow interval monochromatic procedures, collectively referred to as monochromatic procedures.² A brief review of the monochromatic procedures is presented in the following section. The discussion continues by reviewing the correlated k -distribution method and the associated exponential sum-fitting of transmission (ESFT) technique. The following section details the formulation of an efficient yet highly accurate parameterization of the CKD-2.1 continuum code.⁵ The parameterized continuum code captures the accuracy of the CKD-2.1 continuum code while maintaining the efficiency and transportability of previous water vapor continuum codes.⁶ To establish the accuracy of the correlated k -distribution routines, comparisons of flux calculations have been made to reference monochromatic calculations. The results of the model comparisons are summarized in the final section.

2. MOLECULAR LINE ABSORPTION

The most important molecular absorption features located within the spectral range of the CERES window channel have been attributed to H_2O and O_3 . There are, however, several minor trace gases, most notably CO_2 , N_2O , CH_4 , CFC-11, CFC-12 and HCFC-22, that possess important absorption features within the 835 to 1250 cm^{-1} spectral range. The distribution of molecular absorption features within the CERES window channel is highly nonuniform. Thus, to ensure highly accurate parameterizations, it has been necessary to subdivide the 835–1250 cm^{-1} spectral range into three subintervals (see Table 1). The first subinterval, the 835–980 cm^{-1} spectral range, is

Table 1. Compilation of the trace gas species considered for each of the CERES window channel subintervals.

ω_0	ω_f	H ₂ O	CO ₂	O ₃	N ₂ O	CH ₄	CFC-11	CFC-12	CFC-22
835	980	X	X				X	X	X
980	1100	X	X	X			X	X	X
1100	1250	X		X	X	X	X	X	X

dominated by H₂O absorption, although a smaller yet significant contribution from the 10.4 μm band of CO₂ is also present. For the subinterval covering the 980–1100 cm^{-1} spectral range, the upwelling TOA flux is dominated by the 9.6 μm band of O₃ while the downwelling surface flux is dominated by H₂O absorption. CO₂ also contributes a small yet significant absorption within the 980–1100 cm^{-1} spectral range. The most prominent absorption in the subinterval covering the 1100–1250 cm^{-1} spectral range is attributed to H₂O, although significant absorption is also contributed by O₃, N₂O and CH₄. In addition, the chlorofluorocarbons, CFC-11, CFC-12 and HCFC-22, possess relatively weak but important absorption features which pervade the entire spectral range of the CERES window channel.

2.1. The monochromatic procedure

The line-by-line, or monochromatic, procedure is currently the most rigorous approach for theoretically obtaining the absorption coefficient of a particular molecular species. For molecular species whose line structures are resolvable, the absorption coefficient may be expressed as

$$k_{\omega}(p, \theta) = \sum_i S_i(\theta) f_{i, \omega}(p, \theta), \quad (1)$$

where ω is the wavenumber, p is the pressure, θ is the temperature, $S_i(\theta)$ is the intensity of the i th line, and $f_{i, \omega}(p, \theta)$ is the line shape factor. The temperature dependence of the line intensities, as obtained from quantum theory, is given by

$$S(\theta) = S_0 \frac{Z_{\omega}(\theta_0)}{Z_{\omega}(\theta)} \left(\frac{\theta_0}{\theta} \right)^m \exp \left[\frac{hc}{b_k} E'' \left(\frac{1}{\theta_0} - \frac{1}{\theta} \right) \right], \quad (2)$$

where h is Planck's constant, c is the speed of light, b_k is Boltzmann's constant, E'' is the energy of the lower state, Z_{ω} is the vibrational partition function, S_0 is the line intensity at $\theta_0 = 296$ K, and m is the exponent for the temperature dependence of the rotational partition function. The value of m is taken to be 1.0 for the linear molecules CO₂ and N₂O, 1.5 for the asymmetric top molecules H₂O and O₃, and 1.5 for the spherical top molecule CH₄. The pressure and temperature dependence of the air-broadened Lorentz half-width is given by

$$\gamma_i = \gamma_i^0 \left(\frac{p}{p_0} \right) \left(\frac{\theta_0}{\theta} \right)^n \quad (3)$$

for each line, where γ_i^0 is the half-width of the i th line, $p_0 = 1$ atm and $\theta_0 = 296$ K. The exponent n of the temperature dependence of the Lorentz half-width is taken to be 0.62 for H₂O, 0.72 for O₃, 0.77 for CO₂, 0.75 for N₂O and 1.00 for CH₄.⁷ For present purposes, the line shape factor is determined by utilizing Schreier's⁸ vectorized formulation of the Humlíček⁹ Voigt algorithm. Each Voigt line is taken to have a line cutoff of 256 times the Lorentz half-width or 5 times the Doppler half-width, whichever is greater. As a consequence of the current cutoff criteria, approximately 0.25% of the integrated intensity of the Voigt line is not included in the calculation. The line locations, intensities, air-broadened Lorentz half-widths, and lower state energies for H₂O, CO₂, O₃, N₂O and CH₄ are taken from the 1992 version of the air force geophysics laboratory (AFGL) HITRAN database.⁷ The absorption coefficients have been computed with a spectral resolution of 0.005 cm^{-1} , a resolution which ensures accurate absorption coefficient calculations well into the stratosphere.²

As noted previously, in addition to H₂O, CO₂, O₃, N₂O and CH₄, the molecular species CFC-11, CFC-12 and HCFC-22 also possess radiatively important absorption bands within the spectral range of the CERES window channel.^{10,11} For conditions encountered in the earth's troposphere

and stratosphere, however, the absorption bands of the CFC-11, CFC-12 and HCFC-22 are characterized by an extremely dense line structure with line spacings that are significantly smaller than the line half-widths.^{12,13} Thus, the rotational fine structure of the bands is smeared-out and the spectral absorption coefficients become slowly varying functions with wavenumber.¹⁴ Since the CFC absorption coefficients are in the smeared-out line structure limit, the use of the detailed line-by-line procedure is not warranted. Instead, it is more appropriate to use laboratory measured absorption coefficients which can be incorporated by a narrow interval monochromatic procedure. For atmospheric modeling, Kratz and Varanasi¹⁵ concluded that a wavenumber resolution of 0.5 cm^{-1} is sufficient to yield highly accurate results. The present study uses the monochromatic procedure detailed in Kratz and Varanasi¹⁵ along with the laboratory measured absorption coefficients of Varanasi.^{12,13} The CFC bands used in the present study are presented in Table 1 of Kratz et al.¹⁰

The monochromatic procedure (either the line-by-line procedure or the narrow interval monochromatic procedure used for the CFCs) may be integrated over a given spectral interval $\Delta\omega$, for a column abundance u , to yield the spectral-mean transmission $T_{\Delta\omega}(u, p, \theta)$, which may be expressed as

$$T_{\Delta\omega}(u, p, \theta) = \int_{\Delta\omega} \exp[-k_{\omega}(p, \theta)u] \frac{d\omega}{\Delta\omega}. \quad (4)$$

Thus, the results of the monochromatic calculations are given very precisely, with accuracies limited only to the extent of our knowledge of the physical processes involved and of the various input parameters utilized in the calculations. Such precision for the monochromatic calculations requires a substantial fraction of the computing resources. Considering the number of other physical processes that must be taken into account by retrieval algorithms applied to the enormous amounts of data produced by satellites, it is impractical to dedicate so much time to molecular absorption. Nevertheless, the monochromatic procedure is extremely useful both as a tool in parameterizing the observed molecular absorption and as a reference against which to compare the various less-detailed models.

2.2. The correlated k -distribution procedure and exponential-sum fitting

For pressures and temperatures characteristic of the earth's troposphere and stratosphere, the spectra of most absorbing gases are characterized by highly complex distributions of absorption coefficient $k_{\omega}(p, \theta)$ with wavenumber ω (see Fig. 2a). Even the spectra of the CFC's are relatively complex^{12,13} despite having line structures that are smeared-out by extremely narrow line spacings. As previously noted, the monochromatic procedure retraces the complex relationship between absorption coefficient and wavenumber with sufficient spectral resolution to accurately reproduce the spectrum of absorption coefficients. An examination of the relationship of the absorption coefficients versus wavenumber, however, reveals that similar values of $k(p, \theta)$ reoccur frequently. Thus, the computational efficiency can be dramatically improved by substituting the integration over wavenumber by an integration over $g(k)$, the cumulative probability function of the absorption coefficient.^{1,16,17} The function $g(k)$ is defined so that $g(k) dk$ represents the cumulative fraction of the spectral interval contained between the absorption coefficient values of k and $k + dk$. The resulting monotonic dependence of $T_{\Delta\omega}(u, p, \theta)$ upon $g(k)$ (see the smooth curve in Fig. 2b) leads to the concept of the k -distribution method.¹⁸⁻²⁰ The spectral-mean transmission from Eq. (4) can therefore be rewritten as

$$T_{\Delta\omega}(u, p, \theta) = \int_0^1 \exp[-k_g(p, \theta)u] dg. \quad (5)$$

The transformation of the k -distribution from ω space to g space results in an increase in the computational efficiency which is dependent not only upon the relative resolutions taken for ω and g spaces, but also upon the fact that most line-by-line calculations incorporate the contributions of many lines into each integration point within the $\Delta\omega$ interval. During the transformation process, the principal tradeoff for the increased efficiency is the loss of the precise wavenumber location of the k values; however, the loss of this information is not crucial for the retrieval of CERES window

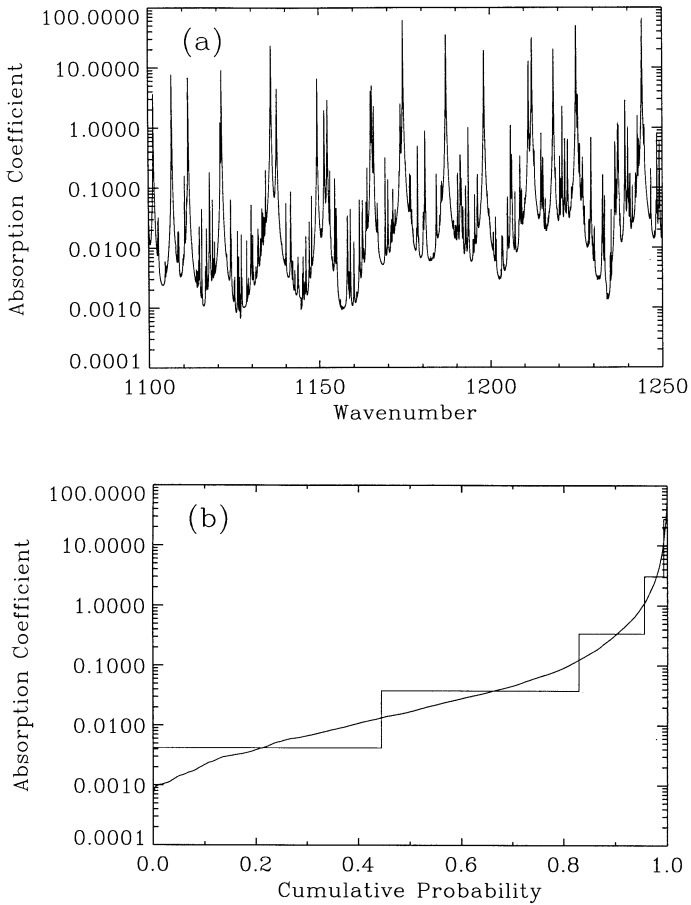


Fig. 2. Absorption coefficient, k , in units of $\text{cm}^{-1} (\text{g cm}^{-2})^{-1}$ as a function of (a) wavenumber and (b) cumulative probability for H_2O absorption at a pressure of 500 hPa and a temperature of 250 K for the wavenumber interval of 1100–1250 cm^{-1} .

channel radiances. For calculations involving tropospheric and stratospheric pressures, a g space resolution of 0.001 has proven to be very accurate.² While significant, the increase in computational speed afforded by the transformation from ω to g space, with a resolution of order 0.001, is still insufficient for use in satellite retrieval calculations. Further arbitrary reductions in the g space resolution may, however, compromise the accuracy of the model calculation. Thus, it is necessary to devise a method whereby the optimal number of k values can be obtained for a specified accuracy. Such an optimization method, known as the exponential-sum fitting of transmissions (ESFT), was first applied by Hunt and Grant²¹ to examine infrared absorbing-scattering problems involving cirrus clouds. The ESFT method has subsequently been utilized for calculations involving a variety of atmospheric conditions (see references in Ref. 2). The application of the ESFT method effectively replaces the spectral-mean transmission from Eq. (5) by a fit to a sum of exponentials:

$$T_{\Delta\omega}(u, p, \theta) \simeq \sum_{i=1}^N w_i \exp[-k_i(p, \theta)u]. \quad (6)$$

Thus, $T_{\Delta\omega}(u, p, \theta)$ is approximated by a summation over N monochromatic calculations corresponding to the absorption coefficients $k_i(p, \theta)$ and weights w_i (see the stepped curve in Fig. 2b). The physical interpretation of the terms $k_i(p, \theta)$ and w_i give rise to the requirements: $k_i(p, \theta) \geq 0$ and $w_i > 0$. Moreover, because the transmission function must asymptote to 1 as the molecular abundance approaches 0, the summation over the weights is constrained by

$$\sum_{i=1}^N w_i = 1. \quad (7)$$

The present study employs the ESFT procedure of Kratz² to derive the $k_i(p, \theta)$ coefficients used in the CERES window channel retrieval algorithms. The discussion in Kratz² contains a thorough step-by-step description of an ESFT procedure which utilizes the least-squares procedure of Press et al.²² and which can be used to construct k -distributions that represent the molecular absorption associated with any specified spectral interval. In this ESFT procedure the values of $k_i(p, \theta)$ are selected *a priori* to be constrained by the relationship

$$k_i(p, \theta) = nk_{i-1}(p, \theta), \quad (8)$$

where n is a positive integer. Thus, each of the exponential terms can be derived from the previous $k_i(p, \theta)$. This ESFT procedure has proven to be very useful in the derivation of the $k_i(p, \theta)$ coefficients necessary for k -distribution routines used by satellite retrieval algorithms.² Furthermore, this ESFT procedure is notable in that it produces $k_i(p, \theta)$ coefficients which represent a realistic distribution of k with $g(k)$ as can be seen by comparing the stepped curve to the smooth curve in Fig. 2b.

To account for the nonhomogeneity of the atmosphere the present model incorporates the assumption that the transformation of a distribution of absorption coefficients from wavenumber space to cumulative probability space will always result in an absorption coefficient, $k_\omega(p, \theta)$, retaining the same cumulative probability regardless of pressure and temperature. Thus, $k_\omega(p, \theta)$ is assumed to always map into the same $k_g(p, \theta)$ regardless of pressure and temperature. This direct correlation between absorption coefficient and cumulative probability gives rise to the concept of the correlated k -distribution. Fu and Liou¹ have investigated the mathematical and physical conditions under which the correlated k -distribution method is applicable, and have found that the assumption of correlation is sufficiently accurate for most atmospheric radiative transfer applications. Since the absorption coefficients are taken to be correlated for all pressure and temperature, the correlated k -distribution procedure can be calculated through a nonhomogeneous atmosphere in the same manner as a monochromatic calculation.

Because the correlated k -distribution method assumes that the distribution of k values for any pressure and temperature are correlated with the distribution of k values determined at the reference pressure and temperature, then each of the sets of monochromatically generated absorption coefficients can then be sorted and binned with precisely the same distribution as was accomplished for the reference pressure and temperature. In order to provide a mechanism to obtain the k -coefficients for the pressures and temperatures representative of the Earth's atmosphere, the monochromatic procedure was employed to obtain the k -coefficients at 19 pressures with $\Delta \log_{10} p = 0.2$ along with three temperatures (210, 250 and 290 K). This choice of $\Delta \log_{10} p = 0.2$ for the pressure levels²³ results in negligibly small errors in the calculation of spectrally averaged k -coefficients when used in conjunction with the linear interpolation of pressures given by

$$k_i(p, \theta_r) = k_i' + (k_i'' - k_i')(p - p')/(p'' - p'), \quad (9)$$

where k_i' and k_i'' are the k_i values precomputed at pressures p' and p'' , respectively, for the reference temperature, θ_r , which is taken to be 250 K. To improve the accuracy of the correlated k -distribution procedure, a linear adjustment to the values of the k_i 's was made at each of the 57 (19×3) pressure and temperature combinations. The motivation for this linear adjustment, which is primarily affected by the pressure, is illustrated by Fig. 4a of Fu and Liou¹ and Fig. 5 of Chou et al.²⁴ The most noticeable effect of this linear adjustment are improvements in the cooling rates for pressures far from the reference pressure. The temperature dependence of the absorption coefficients can be adequately reproduced for the typical range of atmospheric temperatures by a quadratic in $k(p, \theta)$.²⁵

$$k_i(p, \theta) = k_i(p, \theta_r) + a_i(\theta - \theta_r) + b_i(\theta - \theta_r)^2, \quad (10)$$

where the coefficients a_i and b_i have been determined from the k_i values at temperatures $\theta = 210, 250$ and 290 K for each pressure p . Once the correlated k values are calculated for the predetermined set of pressures and temperatures, the interpolation procedures of Eqs. (9) and (10) can then be used to determine the coefficient's pressure and temperature dependence. Thus, for the correlated

k -distribution method, the transmittance for a nonhomogeneous layer between altitudes z' and z'' is given by

$$T_{\Delta\omega}(z', z'') \simeq \sum_{i=1}^N w_i \exp \left[- \int_{z'}^{z''} k_i(p, \theta) \rho dz \right], \quad (11)$$

where $k_i(p, \theta)$ is derived from Eqs. (9) and (10), and ρ is the density of the absorber.

Frequently, the absorption within a spectral interval arises from a combination of overlapping absorption features from several molecular species. The importance of properly considering the radiative impact of this overlap phenomenon has been well established²⁶ and several techniques have been devised to account for the overlap of absorption features. The standard procedure to account for the overlap of the spectral features of different molecular species is the multiplication transmissivity property²⁷ which inherently assumes that the spectral features of the different molecular species are uncorrelated with one another. The spectral mean transmittance for the combination of any two different molecular species can therefore be expressed in terms of the double summation

$$T_{\Delta\omega}(z', z'') \simeq \sum_{i=1}^N \sum_{j=1}^M w_i w_j \exp [-\tau_i(z', z'') - \tau_j(z', z'')], \quad (12)$$

where N and M denote the number of k values, i and j denote the individual coefficients for the different molecular species, and the optical depth for each molecular species is given by

$$\tau_i(z', z'') = \int_{z'}^{z''} k_i(p, \theta) \rho dz. \quad (13)$$

To establish the accuracy of the correlated k -distribution routines as compared with the reference monochromatic procedures, radiative transfer calculations have been performed for a wide variety of atmospheric conditions. The present calculations have utilized the updated versions of the McClatchey et al²⁸ atmospheres as reported by Ellingson et al.²⁹ The vertical resolutions within the atmospheric profiles were taken to be 1 km from the surface to 25 km, and 5 km from 25 km to the top of the atmosphere (70 km). Since this study is focused upon the radiative effects of molecular absorption for the clear-sky case, the radiative effects of clouds and aerosol layers are not considered, and the surface emissivity is taken to be unity. The H₂O and O₃ abundances are taken to follow the atmospheric profiles given in Ellingson et al.²⁹ The remaining trace gases have been taken to have the following mixing ratios: 350 ppmv for CO₂, 310 ppbv for N₂O, 1.75 ppmv for CH₄, 0.268 ppbv for CFC-11, 0.503 ppbv for CFC-12 and 0.105 ppbv for HCFC-22, which corresponds to the 1992 abundances.³⁰ To be consistent with the observations of Fabian et al,³¹ the CFC mixing ratios have been taken to decrease with altitude according to the method suggested by Kratz et al.¹⁰

The flux $F_{\Delta\omega}(z)$ for the wavenumber interval $\Delta\omega$ at altitude z is taken to be positive in the direction of increasing altitude and may be written as

$$\begin{aligned} F_{\Delta\omega}(z) = & 2\pi B_{\Delta\omega}(\theta_s) \int_0^1 T_{\Delta\omega}[z; \mu] \mu d\mu + 2\pi \int_0^1 \int_0^z B_{\Delta\omega}(\theta) dT_{\Delta\omega}[z', z; \mu] \mu d\mu \\ & + 2\pi \int_0^1 \int_z^{z_\infty} B_{\Delta\omega}(\theta) dT_{\Delta\omega}[z, z'; \mu] \mu d\mu. \end{aligned} \quad (14)$$

The terms in Eq. (14) not previously defined include the Planck function $B_{\Delta\omega}$, the surface temperature θ_s , the altitude taken for the top of the atmosphere z_∞ , the altitude integration variable z' , and the cosine of the zenith angle μ . As written, Eq. (14) applies directly to the k -distribution model with $B_{\Delta\omega}$ being evaluated at the band center. Whereas for the monochromatic procedure, Eq. (14) represents the integration over the spectral interval of the monochromatic terms. Hemispherical averaging is accomplished using an eight-point Gaussian quadrature.

A comparison of the results from the correlated k -distribution to the monochromatic calculation is presented in Table 2 for $\Delta F^\uparrow(70)$, the reduction in the upward radiative flux at the top of the atmosphere (taken to be 70 km), $F^\uparrow(70)$, the upward flux at the top of the atmosphere, and $\Delta F^\uparrow(0)$,

Table 2. Comparison of the monochromatic line-by-line procedure (LbL) to the correlated k -distribution procedure (ckd) for the case where only the molecular line absorption is considered. $\Delta F^\uparrow(70)$ is the reduction in the upward flux at the top of the atmosphere (taken to be 70 km), $F^\uparrow(70)$ is the upward flux at the top of the atmosphere, and $\Delta F^\downarrow(0)$ is the enhancement to the downward radiative flux at the surface. The calculations utilized the McClatchey et al²⁸ MLS profile. The spectral range is given in units of cm^{-1} while the fluxes are given in units of Wm^{-2}

Interval	Model	$\Delta F^\uparrow(70)$	$F^\uparrow(70)$	$\Delta F^\downarrow(0)$
835–980	LbL	1.278	47.032	5.908
	ckd	1.262	47.075	5.934
980–1100	LbL	8.812	22.520	7.370
	ckd	8.612	22.691	7.374
1100–1250	LbL	3.711	25.442	10.179
	ckd	3.749	25.309	10.473
835–1250	LbL	13.801	94.994	23.457
	ckd	13.623	95.075	23.781

the enhancement to the downward radiative flux at the surface. While the fluxes have been calculated for the full range of McClatchey et al²⁸ atmospheres, the results of the intercomparison of the calculations is quite similar for each of the atmospheres. Thus for brevity, only the results for the McClatchey et al²⁸ midlatitude summer (MLS) atmosphere are reported in Table 2. An examination of the results reported in Table 2 reveals that the present correlated k -distribution routines have the capability of representing the molecular line absorption for the entire CERES window channel with an accuracy that is better than 1.4% for both $\Delta F^\uparrow(70)$ and $\Delta F^\downarrow(0)$. More importantly, however, the present correlated k -distribution routines for the CERES window channel have the capability of representing the outgoing TOA flux, which is analogous to the energy received by a satellite instrument, to an accuracy better than 0.1%. Thus, the present correlated k -distribution routines yield very accurate representations of the molecular line absorption located within the wavenumber range of the CERES window channel.

3. THE PARAMETERIZED CKD-2.1 CONTINUUM

Within the spectral range of the CERES window channel, the absorption attributed to H_2O is characterized both by individual lines and a continuum. Although radiatively important, the H_2O continuum has a wavenumber-dependent intensity that has proven difficult to measure, and a nature that continues to be controversial.^{11,32,33} Despite the uncertainties surrounding the H_2O continuum, many climate models³⁴ have relied upon the empirical formulation of Roberts et al⁶ to account for the continuum's radiative effect within the spectral range of the 8–12 μm window region. Nevertheless, a more accurate representation of the H_2O continuum has become available through the use of the CKD-2.1 continuum code.^{5,11} The sheer size and complexity of CKD-2.1 continuum code, however, is not conducive to its use in complex parameterized climate and satellite retrieval algorithms. Moreover, as compared to the Roberts et al⁶ continuum formulation, the CKD-2.1 continuum code produces a substantial enhancement to the computational burden. Thus, efficient, yet accurate parameterizations of the CKD-2.1 continuum code have been created for the spectral intervals corresponding to the CERES window channel as well as for several additional spectral intervals of interest to the CERES endeavor.

To create the parameterized CKD-2.1 continuum routines (hereafter the P-CKD routines) for the three subintervals which constitute the CERES window channel, the following steps were taken. A set of values for H_2O amount, pressure, temperature, and pathlength are selected to encompass the expected variation found in the atmosphere. From this set, the secondary input of partial pressure due to H_2O is determined. The range of each parameter is as follows: for H_2O amount 10^{-10} – 10^2 (g cm^{-2}), for pressure 100–1000 hPa, for temperature 200–320 K, and for layer thickness 0.25–1.50 km. Within the selected range of parameters, only the combinations that produce relative

humidity in the range 0.5% to 110% have been included. The result is a set of 7829 unique atmospheric states. For present purposes the volumetric mixing ratios of the principal atmospheric gases is taken to be: 0.78084 for N₂, 0.20948 for O₂, and 0.00934 for Ar. The CKD-2.1 continuum code was then run for each CERES window channel subinterval at a 5 cm⁻¹ wavenumber resolution with the optical depths being averaged over each wavenumber interval. Two methods of averaging were considered: linear and logarithmic. For the subintervals which constitute the CERES window channel, the linear averaging procedure has yielded higher accuracies and thus has been used in the present study. For each subinterval, the subset of optical depth values that was passed to the regression package has been limited to a range of ln(τ) from -4 to 2 (or τ from 0.018 to 7.38). The regression package employed to obtain the present parameterization coefficients is the PV-WAVE software function REGRESS which is based upon the program REGRES in Bevington.³⁵ The multiple linear regression of the H₂O continuum results in an equation of the form

$$\ln(\tau) = a_0 + a_1 \ln(u) + a_2 \theta + a_3 p + a_4 e + a_5 u + a_6 \ln(e), \quad (15)$$

where the previously undefined terms include the a_n 's which are the regression coefficients, and e which is the partial pressure due to H₂O. The values of regression coefficients for Eq. (15) for the CERES window channel subintervals are presented in Table 3. The relative importance of each variable has been determined by examining the improvement in the root-mean-square error between the input value and regression result as each term was introduced. For the CERES window channel subintervals, the use of just the first four terms in Eq (15) yields satisfactory results. It has been noted, however, that for spectral intervals outside the 670–1250 cm⁻¹ range, the additional terms a_5 and a_6 contribute significantly. For each of the CERES window channel subintervals, the root-mean-square error has been observed to be 0.02% for the stated range of optical depths.

A comparison of the results of the P-CKD formulation as used by the correlated k -distribution procedure to the CKD-2.1 continuum code as used by both the monochromatic and the correlated k -distribution procedures is presented in Table 4. As previously with Table 2, the results in Table 4 are reported only for the McClatchey et al²⁸ MLS atmosphere. An examination of the results

Table 3. Coefficients for the parameterization of the CKD-2.1 continuum code for the CERES window channel subintervals

$\Delta\omega$	a_0	a_1	a_2	a_3	a_4	a_5	a_6
835–980	9.387	1.000	-0.02441	0.02154	-0.7674	-5.568×10^{-6}	0.9903
980–1100	8.436	1.000	-0.02324	0.02087	-0.8128	1.466×10^{-5}	0.9934
1100–1250	7.213	1.001	-0.02031	0.05695	-0.4606	-4.432×10^{-4}	0.9602

Table 4. Same as Table 2 except the comparison is for the case where only the H₂O continuum is considered and the comparison is among the monochromatic line-by-line procedure using the CKD-2.1 code (LbL), the correlated k -distribution procedure using the CKD-2.1 code (ckd(1)) and the correlated k -distribution procedure using the P-CKD code (ckd(2))

Interval	Model	$\Delta F^\uparrow(70)$	$F^\uparrow(70)$	$\Delta F^\downarrow(0)$
835–980	LbL	1.838	46.473	18.325
	ckd(1)	1.849	46.488	18.342
	ckd(2)	1.844	46.492	18.312
980–1100	LbL	0.781	30.551	7.300
	ckd(1)	0.780	30.522	7.261
	ckd(2)	0.781	30.521	7.272
1100–1250	LbL	0.675	28.479	5.663
	ckd(1)	0.674	28.384	5.651
	ckd(2)	0.678	28.380	5.706
835–1250	LbL	3.314	105.503	31.288
	ckd(1)	3.303	105.394	31.254
	ckd(2)	3.303	105.393	31.291

presented in Table 4 reveals that the P-CKD procedure reproduces the results of the CKD-2.1 continuum code with an extremely high accuracy (better than 0.1%). The only notable discrepancy among the results presented in Table 4 has been attributed to the change in the spectral resolution from the monochromatic procedure to the correlated k -distribution procedure. Even then, the accuracy of the P-CKD formulation is better than 0.4% for $F^\uparrow(70)$, and 0.1% for $\Delta F^\uparrow(70)$ and $\Delta F^\downarrow(0)$. The most crucial result, of course, is the ability of the P-CKD routines to represent the outgoing TOA flux to an accuracy that is better than 0.1%. Thus, the P-CKD routines very accurately represent the H₂O continuum located within the wavenumber range of the CERES window channel.

4. MODEL RESULTS AND CONCLUSIONS

The results presented in the previous two sections have demonstrated that for the CERES window channel the correlated k -distribution routines accurately reproduce the molecular line absorption as calculated by the monochromatic procedures, and that the P-CKD formulations accurately reproduce the infrared H₂O continuum as calculated by the CKD-2.1 continuum code. In order to establish the accuracy of the calculations which consider the combined effect of these processes, model calculations have also been performed for the case where both the molecular line absorption and H₂O continuum have been computed simultaneously. A comparison of the results is presented in Table 5 for the combined line absorption and continuum calculations for the McClatchey et al²⁸ MLS atmosphere. An examination of the results reported in Table 5 reveals that the present correlated k -distribution routines in conjunction with the P-CKD formulation have the capability of representing the molecular line and continuum absorption for the entire CERES window channel with an accuracy of better than 1.2% for $\Delta F^\uparrow(70)$ and 0.5% for $\Delta F^\downarrow(0)$. More importantly, however, the present correlated k -distribution routines for the CERES window channel have the capability of representing the outgoing TOA flux to an accuracy better than 0.1%. Thus, the present correlated k -distribution routines in conjunction with the P-CKD formulation yield very accurate representations of the combined molecular line and continuum absorption located within the wavenumber range of the CERES window channel. It should be noted that the computational burden encountered by adding the P-CKD formulation to the correlated k -distribution routines is quite small, of order 1%. In contrast, the computational burden encountered by adding the CKD-2.1 continuum code to the correlated k -distribution routines is quite large, in one case doubling the computing time.

For the calculations that have been discussed so far, it has been assumed that the spectral response function is unity for the CERES window channel. An examination of Fig. 1, however, reveals that the CERES window channel response function is not unity and furthermore possesses a notable wave number dependence. Thus, it is necessary to compare the results of the correlated k -distribution to the reference monochromatic calculations for the cases where the response function is considered.

Table 5. Same as Tables 2 and 4 except that the comparison is for the case where all of the infrared active trace gases with spectral features within the CERES window channel are considered

Interval	Model	$\Delta F^\uparrow(70)$	$F^\uparrow(70)$	$\Delta F^\downarrow(0)$
835–980	LbL	2.915	45.396	21.536
	ckd(1)	2.881	45.455	21.533
	ckd(2)	2.877	45.459	21.507
980–1100	LbL	9.221	22.111	12.573
	ckd(1)	9.016	22.286	12.480
	ckd(2)	9.016	22.286	12.489
1100–1250	LbL	4.109	25.044	13.382
	cdk(1)	4.158	24.900	13.688
	cdk(2)	4.160	24.898	13.720
835–1250	LbL	16.245	92.551	47.491
	cdk(1)	16.055	92.641	47.701
	ckd(2)	16.053	92.643	47.716

Because the correlated k -distribution procedure ignores the wavenumber dependence of the absorption coefficients, it is necessary to approximate the spectral response function by an average value for each spectral interval. Kratz² has found that the square-wave approximation to the satellite response function can yield very accurate results whenever there is a lack of correlation between the wavenumber dependence of the absorption coefficient distribution and the spectral response function. With one exception the molecular absorption bands located within the 835–1250 cm^{-1} spectral range possess very little correlation to the CERES window channel response function. The notable exception is located within the 1100–1250 cm^{-1} subinterval, where the CH_4 absorption is anti-correlated with both the CERES window channel spectral response function and the Planck function. Applying the response function to the correlated k -distribution routine for the 1100–1250 cm^{-1} subinterval leads to a substantial overestimation of the radiative impact of CH_4 . This problem has been alleviated by creating a k -distribution for CH_4 which is specifically tailored for use with the CERES window channel spectral response function. Unlike the k -distribution created for CH_4 in Sec. 3 which considered the contributions of all the lines within the 1100–1250 cm^{-1} spectral interval, the new k -distribution considers only the contributions of the lines within the half-power points of the response function. The k -distribution is thus created for a subset of the CH_4 lines, with the k -values being renormalized to account for the change in the extent of the spectral interval. With this k -distribution the radiative effect of the CH_4 can be estimated within a few percent for the case where the CERES window response function is considered. It must be noted, however, that the revised CH_4 routine is intended only to be employed in conjunction with the CERES window channel response function.

In order to determine the accuracy of the correlated k -distribution algorithms incorporating the CERES window channel response function, a comparison of the results of the combined line absorption and continuum calculations is presented in Table 6 for conditions identical to Table 5 except that the CERES window channel response function has been taken into account. From an examination of the comparisons presented in Table 6, it is found that despite the added complexity of the response function, the accuracies of the correlated k -distribution calculations relative to the monochromatic calculations are quite similar to those presented in Table 5. Indeed, the present correlated k -distribution routines including the CERES window channel response function have the capability of representing the outgoing TOA flux to an accuracy better than 0.1%. Therefore, the incorporation of the response function does not compromise the accuracy of the present correlated k -distribution routines.

As an additional check of the accuracy of the correlated k -distribution algorithms which incorporate the CERES window channel response function, calculations were performed not only for the five McClatchey et al²⁸ profiles but also for an additional 45 atmospheric profiles representative of the latitudinal range from -30° S to 60° N.³⁶ The results for all 50 cases are presented in Fig. 3 for the upward flux at the top of the atmosphere, $F^\uparrow(70)$. The correlation coefficient between the results of the correlated k -distribution and reference monochromatic models is very high (0.999979), and the

Table 6. Same as Table 5 except that the CERES window channel instrument response function is included in the calculations

Interval	Model	$\Delta F^\uparrow(70)$	$F^\uparrow(70)$	$\Delta F^\uparrow(0)$
835–980	LbL	1.983	31.357	14.593
	ckd(1)	1.987	31.353	14.853
	ckd(2)	1.985	31.356	14.835
980–1100	LbL	7.002	16.773	9.545
	ckd(1)	6.848	16.927	9.479
	ckd(2)	6.848	16.926	9.486
1100–1250	LbL	2.496	16.828	8.482
	cdk(1)	2.596	16.728	8.943
	ckd(2)	2.597	16.726	8.965
835–1250	LbL	11.481	64.958	32.620
	cdk(1)	11.431	65.008	33.275
	ckd(2)	11.430	65.008	33.286

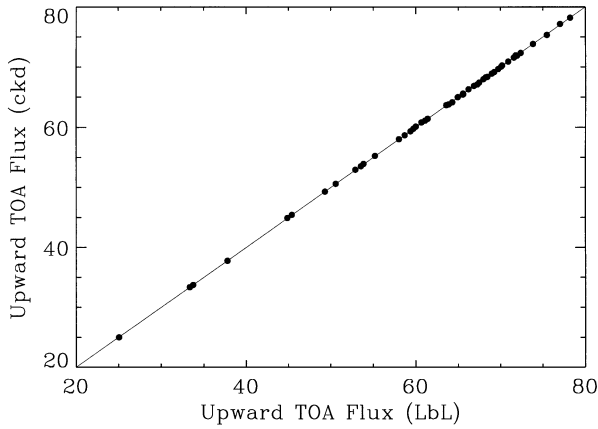


Fig. 3. Comparison of outgoing TOA clear-sky fluxes as computed by the correlated k -distribution (ckd) and monochromatic line-by-line (LbL) models. The values have been computed for the spectral range of the CERES window channel, with the response function taken into consideration, and are given in units of W m^{-2} .

Table 7. Comparison of the correlated k -distribution procedure using the P-CKD code (ckd) for various combinations of the infrared active trace gases to the monochromatic line-by-line procedure using the CKD-2.1 code (LbL) using all of the infrared active trace gases. The brightness temperature, θ_b , which is representative of the TOA flux, is included to elucidate the magnitude of the radiative impact of the trace gases upon the satellite measured radiances. As with Table 6, the CERES window channel instrument response function is included in the calculations

Gases included	Model	ΔF^\uparrow (70)	F^\uparrow (70)	ΔF^\uparrow (0)	θ_b (70)
All	LbL	11.481	64.958	32.620	284.70
All	ckd	11.430	65.008	33.286	284.72
H ₂ O & O ₃	ckd	10.508	65.931	32.132	285.55
H ₂ O only	ckd	4.491	71.948	30.043	290.32
O ₃ only	ckd	6.431	70.008	3.335	289.02
none	ckd	0.000	76.439	0.000	294.00

mean and standard deviation of the ratio of the correlated k -distribution model to the monochromatic procedure is 1.000023 and 0.001158, respectively. Thus, high accuracy has been established for the correlated k -distribution model for a wide variety of atmospheric conditions.

An ancillary question which has been raised concerns the need to include the entire contingent of trace gases in the retrieval algorithms. Calculations have been performed to address this question with the results being presented in Table 7 for conditions identical to Table 6. From Table 7, it is observed that neglecting the contributions from all the species except H₂O and O₃ for the McClatchey et al²⁸ MLS atmosphere yields an upwelling TOA flux of 65.931 W m^{-2} which is a 1.5% overestimation. This 1.5% overestimation in the flux calculations corresponds to an error in the retrieved brightness temperature of 0.85 K. Under circumstance where rapid processing is extremely critical, this error may be deemed acceptable. In contrast, neglecting the contribution from all of the molecular species yields an upwelling TOA flux of 76.439 W m^{-2} , a 17.7% overestimation equivalent to an error in the retrieved brightness temperature of 9.3 K, which is certainly not acceptable but does emphasize the need to account for molecular absorption within the spectral range of the CERES window channel instrument.

The present correlated k -distribution routines in conjunction with the P-CKD formulation yield very accurate representations of the combined molecular line and continuum absorption located within the wavenumber range of the CERES window channel. The CERES endeavor is a critical part of NASA's EOS project, with the TOA radiances measured by the CERES window channel being vital to the retrieval of the surface radiation budget.⁴ In addition, the CERES window channel measurements provide a measure of the trace gas radiative forcing under clear sky conditions. The

correlated k -distributions which have been constructed for the CERES window channel are available from the author by request. Alternatively, the correlated k -distribution routines for the CERES window channel as well as several other satellite channels may be accessed at:

<http://aquila.larc.nasa.gov:8080/>

The P-CKD routines created for the spectral range of the CERES window channel along with P-CKD routines for use with the Fu and Liou¹ bands are also available at:

http://srbsun.larc.nasa.gov/~rose/fu-liou/clough_inabox.f

Acknowledgements—The authors would like to acknowledge the beneficial discussions with A. B. Carlson and T. P. Charlock concerning the preparation of the manuscript. The authors would also like to thank S. K. Gupta for providing the soundings used to produce the results reported in Fig. 3. This research was supported through funding from the NASA Earth Observing System Program.

REFERENCES

1. Fu, Q. and Liou, K. N., *J. Atmos. Sci.*, 1992, **49**, 2139.
2. Kratz, D. P., *JQSRT*, 1995, **53**, 501.
3. Lee, R. B., Barkstrom, B. R., Smith, G. L., Cooper, J. E., Kopia, L. P., Lawrence, R. W., Thomas, S., Pandey, D. K. and Crommelynck, D. A. H., *J. Atmos. Ocean Tech.*, 1996, **13**, 300.
4. Inamdar, A. K. and Ramanathan, V., *NASA RP 1376*, 1995, **3**, 217.
5. Clough, S. A., Kneizys, F. X. and Davies, R. W., *Atmos. Res.*, 1989, **23**, 229.
6. Roberts, R. E., Selby, J. E. A. and Biberman, L. M., *Appl. Opt.*, 1976, **15**, 2085.
7. Rothman, L. S., Gamache, R. R., Tipping, R. H., Rinsland, C. P., Smith, M. A. H., Benner, D. C., Devi, V. M., Flaud, J.-M., Camy-Peyret, C., Perrin, A., Goldman, A., Massie, S. T., Brown, L. R. and Toth, R. A., *JQSRT*, 1992, **48**, 469.
8. Schreier, F., *JQSRT*, 1992, **48**, 743.
9. Humlíček, J., *JQSRT*, 1981, **27**, 437.
10. Kratz, D. P., Chou, M.-D. and Yan, M. M.-H., *J. Climate*, 1993, **6**, 1269.
11. Clough, S. A. and Iacono, M. J., *J. Geophys. Res.*, 1995, **100**, 16 519.
12. Varanasi, P., *JQSRT*, 1992, **48**, 205.
13. Varanasi, P., *JQSRT*, 1992, **47**, 251.
14. Penner, S. S., 1959: *Quantitative Molecular Spectroscopy and Gas Emissivities*, Addison-Wesley, Reading, MA, 1959, 587pp.
15. Kratz, D. P. and Varanasi, P., *JQSRT*, 1992, **48**, 245.
16. Goody, R., West, R., Chen, L. and Crisp, D., *JQSRT*, 1989, **42**, 539.
17. Lácis, A. A. and Oinas, V., *J. Geophys. Res.*, 1991, **96**, 9027.
18. Ambartsumian, V., *Publ. Obs. Astron. Univ. Leningrad.*, 1936, **6**, 7.
19. Arking, A. and Grossman, K., *J. Atmos. Sci.*, 1972, **29**, 937.
20. Wang, W.-C. and Shi, G.-Y., *JQSRT*, 1988, **39**, 387.
21. Hunt, G. and Grant, I., *J. Atmos. Sci.*, 1969, **26**, 963.
22. Press, W. H., Flannery, B. P., Teukolsky, S. A. and Vetterling, W. T., *Numerical Recipes*, Cambridge University Press, New York, 1986, 839pp.
23. Chou, M.-D. and Kouvaris, L., *J. Geophys. Res.*, 1986, **91**, 4047.
24. Chou, M.-D., Ridgway, W. L. and Yan, M. M.-H., *J. Atmos. Sci.*, 1995, **52**, 1159.
25. Rodgers, C. D. and Walshaw, C. D., *Quart. J. Roy. Meteor. Soc.*, 1966, **92**, 67.
26. Wang, W.-C. and Ryan, P. B., *Tellus*, 1983, **35B**, 81.
27. Goody, R. M. and Yung, Y. L., *Atmospheric Radiation, Theoretical Basis*, Oxford University Press, New York, 1989, 519pp.
28. McClatchey, R. A., Fenn, R. W., Selby, J. E., Volz, F. E. and Garing, J. S., *Optical Properties of the Atmosphere* 3rd edition, AFCRL-72-0497, Environmental Research Papers No. 411, Air Force Cambridge Research Laboratory, Bedford, MA, 1972, 108pp.
29. Ellingson, R. G., Ellis, J. and Fels, S., *J. Geophys. Res.*, 1991, **96**, 8929.
30. Intergovernmental Panel on Climate Change, *Climate Change, 1994: radiative forcing of climate change and an evaluation of the IPCC IS92 emission scenarios*, Cambridge University Press, 1995, 339pp.
31. Fabian, P., *Adv. Space Res.*, 1987, **7(9)**, 63.
32. Varanasi, P., *JQSRT*, 1988, **40**, 169.
33. Grant, W. B., *Appl. Opt.*, 1990, **29**, 451.
34. Kiehl, J. T. and Ramanathan, V., *J. Atmos. Sci.*, 1982, **39**, 2923.
35. Bevington, P. R., *Data Reduction and Error Analysis for the Physical Sciences*, McGraw-Hill, New York, 1969, 336pp.
36. Phillips, N., Susskind, J. and L. McMillin, *J. Atmos. Ocean Tech.*, 1988, **5**, 44.